

# Gold Nanoislands Grown on Multiphoton Polymerized Structures as Substrate for Enzymatic Reactions

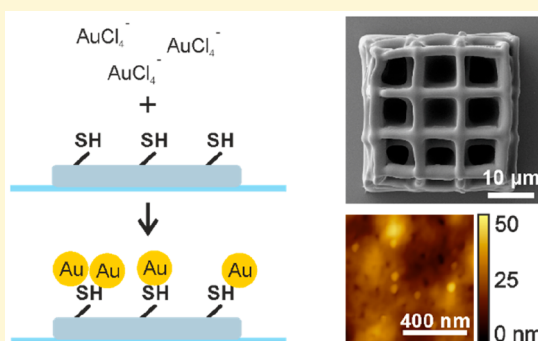
Bianca Buchegger,<sup>\*,§,¶</sup> Cynthia Vidal,<sup>¶</sup> Julia Neuwirth,<sup>§</sup> Boris Buchroithner,<sup>¶</sup> Andreas Karner,<sup>¶</sup> Armin Hochreiner,<sup>¶</sup> Thomas A. Klar,<sup>§,¶</sup> and Jaroslav Jacak<sup>\*,¶</sup>

<sup>§</sup>Institute of Applied Physics, Johannes Kepler University Linz, Altenberger Straße 69, 4040 Linz, Austria

<sup>¶</sup>University of Applied Sciences Upper Austria, School of Medical Engineering and Applied Social Sciences, Garnisonstraße 21, 4020 Linz, Austria

## Supporting Information

**ABSTRACT:** We show that multiphoton thiol–ene polymerized structures comprise unreacted thiol moieties, which can be used for postpolymerization gold metallization. Some of the thiol groups located at the surface are not involved in thiol–ene reactions and, therefore, can serve as nucleation seeds for the synthesis of ~50 nm sized gold nanoislands. Additionally, we show that the nanoislands can be used for immobilization of fluorescent molecules. We observed a significant enhancement of the fluorescence signal on the nanoisland-functionalized polymer structures when compared to the structured polymers without gold. To show a possible application, we bound peroxidase to the gold nanoislands. Peroxidase activity has been verified by chemiluminescence of the converted luminol substrate.



Two- and three-dimensional micro- and nanostructures consisting of metal-functionalized polymers provide enhanced optical and mechanical properties. These attributes have garnered particular attention for their application in the development of metamaterials, biosensors, or implants.<sup>1–5</sup> Advanced three-dimensional fabrication techniques, such as multiphoton polymerization (MPP), enable fabrication of arbitrary structures with feature sizes of ~100 nm and with a resolution down to a few hundred nm by infrared femtosecond (fs)-pulsed lasers.<sup>6–13</sup> Over the last few years, research on noble-metal-containing nanocomposites and metal functionalized polymer structures has gained increased attention and importance.<sup>1–4,14,15</sup> Metals (e.g., silver or gold) have been used as additives in photoresists for MPP for years.<sup>16–19</sup> Recently, two- and three-dimensional metal-containing structures with lateral feature sizes down to 100–200 nm have been realized.<sup>17,19–21</sup> Moreover, rapid progress on the fabrication enabled writing of gold- and silver-doped conductive structures in the micrometer range.<sup>22–24</sup> These metal-functionalized polymers are becoming more commonly utilized as substrates for coatings and molecule immobilization in bioassays.<sup>1,2,25–27</sup> Metals, however, strongly affect the optical properties of structured polymers (e.g. transparency, refractive index) and, therefore, limit the application field of such structures.<sup>5,6</sup>

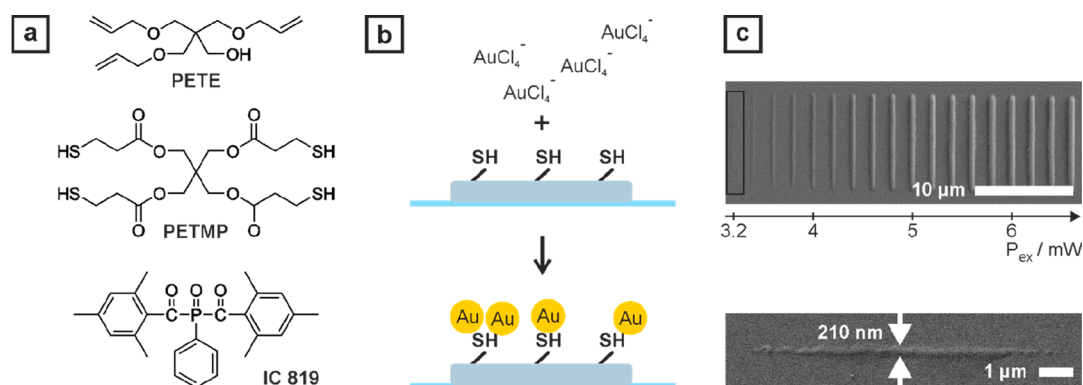
Commonly, methods, such as sputtering, metal evaporation, or electrodeposition, are used to achieve metallization of structured surfaces. These methods either generate homogeneous surface coatings or enable coating of the substrate with randomly immobilized gold nanoparticles (NPs).<sup>7,8</sup> An alternative strategy to metal deposition is the growth of noble metallic NPs on substrates.<sup>28</sup> To date, the synthesis of NPs on polymers has been demonstrated on large scale surfaces (e.g. polydopamine or PDMS)<sup>25,29</sup> and on polyaniline nanofibers.<sup>30</sup> Recently, the growth of silver particles on MPP fabricated structures has also been shown.<sup>24</sup> There are, however, no methods which allow for the growth of gold NPs on the surface of two- and three-dimensionally nanostructured polymeric structures.

In this study, we report a method for the growth of gold nanoislands on top of multiphoton polymerized structures fabricated with a thiol–ene based resin system (chemical structures in Figure 1a) consisting of multifunctional thiols, a multifunctional allylether and a photoinitiator.<sup>31</sup> In the first step, the prefabricated polymeric structures are incubated with an aqueous solution of Au (III) chloric acid (HAuCl<sub>4</sub>) (see

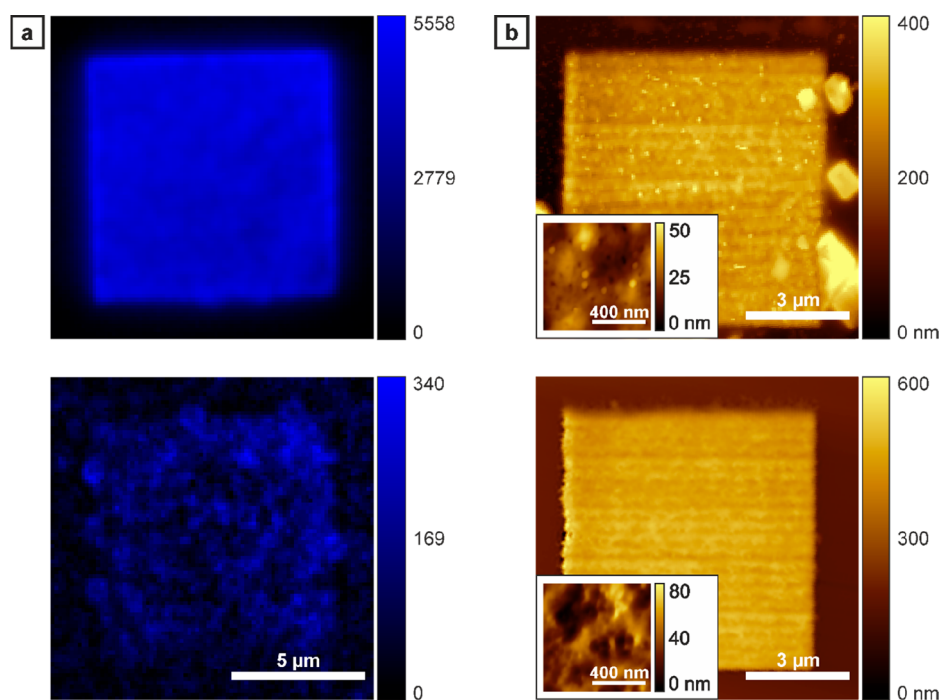
Received: May 24, 2019

Accepted: August 26, 2019

Published: August 26, 2019



**Figure 1.** Components of the thiol–ene based resin, a sketch of the experiment and limitations of fabrication. (a) Chemical formulas of the photoresist ingredients. The monomers PETE and PETMP are mixed in a 1:1 ratio. The photoresist contains 1 wt % Irgacure 819 (IC 819). (b) Sketch of the polymer structures incubated with  $\text{HAuCl}_4$  in deionized water. The thiol groups on the surface of the polymer structures seed the growth of gold nanoislands. (c) Scanning electron microscopy (SEM) images of MPP fabricated lines, written with different excitation powers ( $P_{\text{ex}}$ ) ranging from 3.2–6.6 mW (0.12–0.25  $\text{PW}/\text{cm}^2$ ). The bottom image zoomed in shows a thiol-functionalized polymer line written with 3.2 mW (0.12  $\text{PW}/\text{cm}^2$ ), having a lateral feature size of 210 nm (FWHM). All intensities are measured in front of the objective lens ( $\text{NA} = 1.46$ ).



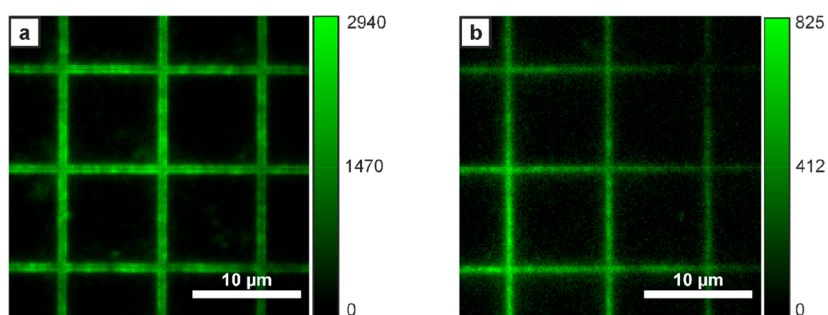
**Figure 2.** Fluorescence and AFM measurements on polymer structures with and without gold nanoislands. (a) Fluorescence images of the polymer structures with gold nanoislands (top) and without gold nanoislands (bottom) post incubation with 1 nM Bodipy FL L-cystine. The fluorescence signal of the structure with gold nanoislands is on average 4662 photons per pixel. The fluorescence signal of the negative control is on average 119 photons per pixel. An excitation wavelength of 491 nm and an illumination time of 5 ms were used for imaging. (b) AFM images of the thiol-functionalized polymer structures with (top) and without (bottom) gold nanoislands. The insets show zoomed-in regions of the polymer surfaces. The top zoomed-in image shows individual nanoislands.

Figure 1b). The randomly distributed thiol functional groups on the surface of the polymeric structures immobilize the gold atoms,<sup>16,17</sup> which form gold nanoislands  $\sim 50$  nm in size. The presence of gold islands is shown via fluorescence and atomic force microscopy (AFM), as well as energy-dispersive X-ray (EDX) spectroscopy.

Figure 1c shows a scanning electron microscopic (SEM) image of MPP written two-dimensional lines. The excitation powers were varied, ranging from 3.2 to 6.6 mW (0.12–0.25  $\text{PW}/\text{cm}^2$ ) in 0.2 mW (7.5  $\text{TW}/\text{cm}^2$ ) increments (the average power was measured before entering an objective lens with

numerical aperture (NA) of 1.46). The smallest written line has a lateral feature size of 210 nm full-width at half maximum (FWHM). Figure S1 demonstrates two- and three-dimensional writing performance of the photoresist. A lateral resolution below 500 nm and an axial resolution of  $\sim 3$   $\mu\text{m}$  can be achieved.

In the next step, cystine-coupled Bodipy fluorophores (Figure S3) were used to characterize the surface binding properties. The dyes attach to the gold nanoislands via thiol-to-gold affinity.<sup>32</sup> The best fluorescence signals, in terms of homogeneity and intensity, were obtained after a 15 min



**Figure 3.** Fluorescence signal from peroxidase–rhodamine isothiocyanate bound to the polymer structures (side length  $63\ \mu\text{m}$ ; grid constant  $9\ \mu\text{m}$ ). (a) The fluorescence signal from the structure with gold nanoislands after incubation with RITC-labeled HRP. The fluorescence signal is on average 1584 counts per pixel. (b) The fluorescence signal of the control structure (without gold nanoislands) equals 343 counts per pixel on average. An excitation wavelength of 532 nm and an illumination time of 1 ms were used for imaging.

incubation of the PETE:PETMP structures with a 50 mM solution of Au(III) chloric acid in deionized water. **Figure 2a** shows fluorescence images of two MPP structured surfaces. The top depicts the fluorescence image of a rectangular structure incubated with 1 nM Bodipy FL *L*-cystine post nanoisland formation. Despite significant fluorescence quenching because of the gold, an average fluorescence signal of 4662 photons per pixel (illumination time 5 ms, pixel size 160 nm) was measured. In **Figure 2a** (bottom), the fluorescence image of a gold untreated structure (negative control) after incubation with 1 nM Bodipy FL *L*-cystine is shown. The determined fluorescence signal of the surface was on average 119 photons per pixel (illumination time 5 ms). Although gold-induced quenching<sup>33</sup> has a significant negative impact on the fluorescence signal, we still measured a  $\sim 40$  fold increased fluorescence signal of the gold-coated structures compared to the negative controls. When taking fluorescence quenching into account, a  $10^3$  times higher fluorophore density of the surface of the gold-coated structure can be expected. Additional fluorescence measurements on two- and three-dimensional structures are shown in the [Supporting Information](#) ([Figures S4](#) and [S5](#)).

For visualization of the gold nanoislands, the structures were imaged via AFM. **Figure 2b** (top) displays images of individual nanoislands on thiol functionalized MPP structured polymers (similar sample preparation as the structure in **Figure 2a** (top)). The zoomed topography data shown in **Figure 2b** (top) visualizes the gold nanoislands randomly distributed on the surface. In comparison, no gold nanoislands were observed in the negative control in **Figure 2b** (bottom). The largest AFM-visualized nanoislands were  $\sim 50$ – $60$  nm. Although not indicated by the AFM data, the presence of additional, smaller gold nanoclusters grown on the polymer structures cannot be excluded.

Additionally, an EDX analysis provides information on the materials' chemical signature. We analyzed the MPP structures including nanoislands, as well as negative control structures. The EDX measurements show 6.42 wt % of gold (0.94 at %) present in the polymer structures with grown gold nanoislands. The negative control shows that there is no gold at the surface of the structures. The EDX spectra are shown in [Figure S7](#).

To show the biotechnological applicability of our structures, we have bound peroxidase (HRP)–rhodamine isothiocyanate (RITC) (Sigma-Aldrich, USA) to the gold nanoislands on the surface of MPP structured polymer grids with a side length of  $63\ \mu\text{m}$  and a grid constant of  $9\ \mu\text{m}$  (**Figure 3**).

Upon interaction of the enzymes' cysteine residues with gold, the proteins are immobilized on the polymer structures. The fluorescence signal of the RITC-labeled HRP on the structures with gold nanoislands equals 1584 counts per pixel on average (**Figure 3a**), whereas the fluorescence signal of the control structures (without gold nanoislands) equals 343 counts per pixel on average due to unspecific binding (**Figure 3b**). Furthermore, an enzymatic activity of the HRP immobilized on the structures has been verified by the chemiluminescence of the converted luminol substrate.

The chemiluminescent signal of the solution enclosing structures with gold nanoislands enhances by a factor of  $\sim 3 \times 10^6$  compared to signal of the solution before incubation ( $1.3 \times 10^{10}$  counts after substrate incubation; 4084 counts before substrate incubation). The signal of the solution originating from the control structures enhances by a factor of  $\sim 3$  (from 1463 counts before substrate incubation to 4765 counts after substrate incubation).

In conclusion, we detail a rapid and simple method for post-polymerization functionalization of MPP written PETE:PETMP structures with gold nanoislands. The nanoislands grown upon treatment with  $\text{HAuCl}_4$  can be used to link molecules to the surface of the gold-coated two- and three-dimensionally structured polymers via thiol-to-gold affinity ([Figures 2a](#) and [S3–S5](#)). This technique has several promising applications including fabrication of biosensors,<sup>34–37</sup> for example, the gold nanoislands can be used to link enzymes for catalysis (**Figure 3**) or proteins, which promote cell adhesion or differentiation. The capability to write structures in three dimensions is beneficial as it increases the surface of the structures and, therefore, the number of gold nanoislands. Further, it is thinkable to use this method in combination with other materials containing thiol groups for MPP.<sup>12,13</sup>

## EXPERIMENTAL PROCEDURES

The photoresist is comprised of two monomers and a photoinitiator. The monomers are a 1:1 mixture of pentaerythritol triallyl ether (PETE, abcr, Germany) and pentaerythritol tetrakis (3-mercaptopropionate) (PETMP, Sigma-Aldrich, USA). The photoinitiator is 1 wt % Irgacure 819 (BASF Schweiz, Switzerland). The chemical structures are shown in [Figure 1a](#). The photoresist was freshly prepared prior to fabrication of the structures. Half a microliter of photoresist was drop-cast on a glass coverslip (no. 1.5, Menzel Gläser, Germany). Polymerization was achieved by focusing a femtosecond, a NIR laser beam (780 nm, 100 fs, 80 MHz repetition rate, Toptica, Germany) into the photoresist using



an oil immersion objective lens ( $\alpha$ -plan apochromat, 100 $\times$ , NA = 1.46, Zeiss, Germany). Thiol functional polymer lines with a length of 10  $\mu\text{m}$  were fabricated using an excitation power of 3.5 mW (0.13 PW/cm<sup>2</sup>). Polymer squares with a side length of 10  $\mu\text{m}$  were typically written using an excitation power of 4 mW (0.15 PW/cm<sup>2</sup>). The given average powers were measured directly before entering the objective lens used to focus the incoming laser pulses into a spot of approximately  $d = 1.22\lambda/\text{NA}$  diameter. The writing speed for structuring was set to 20  $\mu\text{m}/\text{s}$ . A detailed description of the lithography setup can be found for example in ref 11. Post-fabrication, the polymer structures were developed by rinsing with acetone and blown dry with nitrogen. The polymer structures were characterized by SEM after metallization with a 10 nm platinum layer. For EDX spectroscopy, the samples were metallized with a 10 nm platinum layer.

For metallization, the structures were incubated for 15 min with a 50 mM solution of gold(III) chloride hydrate (HAuCl<sub>4</sub>, Sigma-Aldrich, USA) in deionized water; this allowed for growth of the gold nanoislands. The solution was stored at 4° C and used for no more than 24 h. Post incubation, the samples were rinsed with deionized water and ethanol and, then, dried with nitrogen.

Detection of the gold nanoislands on the surface of the polymer structures was carried out using fluorescence microscopy, AFM and EDX spectroscopy. For the fluorescence measurements, the structures were incubated with 1  $\mu\text{L}$  of 1 nM Bodipy FL L-cystine (Thermo Fisher Scientific, USA) in HEPES buffer (50 mM, pH 7.5) for 10 min. To minimize nonspecific binding to the glass substrate, we passivated the substrate by incubating for 20 min with 30  $\mu\text{L}$  of DOPC vesicle solution (1,2-dioleoyl-*sn*-glycero-3-phosphocholine, Avanti Polar Lipids, USA).<sup>38</sup> HEPES was prepared using 0.6 g of 4-(2-hydroxyethyl)-1-piperazineethanesulfonic acid (HEPES, Carl Roth, Germany) in 40 mL of doubly distilled water. After adjusting the pH value to 7.5, water was added to reach a final volume of 50 mL. The buffer solution was stored at 4° C. The binding of the fluorescent molecules to the structures was analyzed via fluorescence microscopy using an excitation wavelength of 491 nm or 532 nm and an illumination time of 5 ms (unless otherwise noted). A detailed description of the fluorescence microscope can be found in refs 37 and 39.

AFM measurements were performed on an Agilent 5400 Scanning Probe Microscope (Keysight Technologies, USA) at room temperature in air. The AFM was operated in contact mode using Bruker MLCT cantilevers (Bruker, USA) with a nominal spring constant of 0.03 N/m. Images were processed using Gwyddion (Czech Metrology Institute, CZ).

To show the possible application of the polymer structures with grown gold nanoislands for biosensors and bioreactors, we structured five two-dimensional grids with a side length of 63  $\mu\text{m}$  and a grid constant of 9  $\mu\text{m}$ . Subsequently to polymer structuring and incubation with a 50 mM solution of gold(III) chloride hydrate, we bound peroxidase (HRP)–rhodamine isothiocyanate (RITC)-labeled (Sigma-Aldrich, USA) to the gold nanoislands on the polymer structures. Thereby, the intrinsic thiolene residues of the cysteine amino acids couple the enzyme to the gold surface.<sup>40</sup> After fabrication and development of the structures, DOPC vesicles were again used to passivate the glass surface. After it was washed with phosphate buffered saline (PBS), we added 2  $\mu\text{L}$  of RITC-labeled HRP (0.01 mg/mL in PBS) for 15 min. After another

washing step with PBS, we added 100  $\mu\text{L}$  of chemiluminescent substrate (1:1 mixture of luminol enhancer and peroxidase buffer, LiteAblotPlus, EuroClone, Italy) to the HRP functionalized structures. After 20 min of HRP activity, 50  $\mu\text{L}$  of the chemiluminescent luminol solution has been analyzed using a spectrophotometer (Infinite M200Pro, Tecan Trading AG, Switzerland). The integration time was set to 100 ms.

## ■ ASSOCIATED CONTENT

### 📄 Supporting Information

The Supporting Information is available free of charge on the ACS Publications website at DOI: 10.1021/acsmaterialslett.9b00182.

Three-dimensional writing capability of the photoresist used for growth of gold nanoislands; fluorescence measurements of two- and three-dimensional polymer structures with grown gold nanoislands; effect of different growth times on nanoisland growth; EDX spectra of polymer structures with and without grown gold nanoislands (PDF)

## ■ AUTHOR INFORMATION

### Corresponding Authors

\*E-mail: bianca.buchegger@jku.at

\*E-mail: jaroslaw.jacak@fh-linz.at

### ORCID

Bianca Buchegger: 0000-0003-4346-8415

Thomas A. Klar: 0000-0002-1339-5844

Jaroslaw Jacak: 0000-0002-4989-1276

### Notes

The authors declare no competing financial interest.

## ■ ACKNOWLEDGMENTS

We would like to thank Bernhard Fragner and Alfred Nimmervoll for technical support and Heidi Piglmayer-Brezina for the EDX and SEM measurements. This work was funded by the Basic Funding of the Upper Austrian University of Applied Sciences Project—PolFunk and the TiMED funding of the Upper Austrian University of Applied Sciences TC-LOEM, the Austria Science Fund (FWF) project P 31827-B21, by the European Fund for Regional Development (EFRE, IWB2020), and by the Federal State of Upper Austria.

## ■ REFERENCES

- (1) Lyon, L. A.; Musick, M. D.; Natan, M. J. Colloidal Au-Enhanced Surface Plasmon Resonance Immunosensing. *Anal. Chem.* **1998**, *70*, 5177–5183.
- (2) Zhang, Q.; Xu, J.-J.; Liu, Y.; Chen, H.-Y. In-situ synthesis of poly(dimethylsiloxane)-gold nanoparticles composite films and its application in microfluidic systems. *Lab Chip* **2008**, *8*, 352–357.
- (3) Saha, K.; Agasti, S. S.; Kim, C.; Li, X.; Rotello, V. M. Gold nanoparticles in chemical and biological sensing. *Chem. Rev.* **2012**, *112*, 2739–2779.
- (4) Hill, R. T. Plasmonic biosensors. *Wires Nanomed Nanobi* **2015**, *7*, 152–168.
- (5) Son, H. Y.; Kim, K. R.; Lee, J. B.; Le Kim, T. H.; Jang, J.; Kim, S. J.; Yoon, M. S.; Kim, J. W.; Nam, Y. S. Bioinspired Synthesis of Mesoporous Gold-silica Hybrid Microspheres as Recyclable Colloidal SERS Substrates. *Sci. Rep.* **2017**, *7*, 14728.
- (6) Maruo, S.; Nakamura, O.; Kawata, S. Three-dimensional microfabrication with two-photon-absorbed photopolymerization. *Opt. Lett.* **1997**, *22*, 132–134.

- (7) Li, L.; Fourkas, J. T. Multiphoton polymerization. *Mater. Today* **2007**, *10*, 30–37.
- (8) Farsari, M.; Vamvakaki, M.; Chichkov, B. N. Multiphoton polymerization of hybrid materials. *J. Opt.* **2010**, *12*, 124001.
- (9) Cicha, K.; Li, Z.; Stadlmann, K.; Ovsianikov, A.; Markut-Kohl, R.; Liska, R.; Stampfl, J. Evaluation of 3D structures fabricated with two-photon-photopolymerization by using FTIR spectroscopy. *J. Appl. Phys.* **2011**, *110*, 064911.
- (10) Fischer, J.; Wegener, M. Three-dimensional direct laser writing inspired by stimulated-emission-depletion microscopy [Invited]. *Opt. Mater. Express* **2011**, *1*, 614–624.
- (11) Wollhofen, R.; Buchegger, B.; Eder, C.; Jacak, J.; Kreutzer, J.; Klar, T. A. Functional photoresists for sub-diffraction stimulated emission depletion lithography. *Opt. Mater. Express* **2017**, *7*, 2538–2559.
- (12) Buchegger, B.; Kreutzer, J.; Plochberger, B.; Wollhofen, R.; Sivun, D.; Jacak, J.; Schütz, G. J.; Schubert, U.; Klar, T. A. Stimulated Emission Depletion Lithography with Mercapto-Functional Polymers. *ACS Nano* **2016**, *10*, 1954–1959.
- (13) Lebedevaite, M.; Ostrauskaite, J.; Skliutas, E.; Malinauskas, M. Photoinitiator Free Resins Composed of Plant-Derived Monomers for the Optical  $\mu$ -3D Printing of Thermosets. *Polymers* **2019**, *11*, 116.
- (14) Malinauskas, A.; Malinauskiene, J.; Ramanavičius, A. Conducting polymer-based nanostructured materials: electrochemical aspects. *Nanotechnology* **2005**, *16*, R51–62.
- (15) Chai, J.; Wong, L. S.; Giam, L.; Mirkin, C. A. Single-molecule protein arrays enabled by scanning probe block copolymer lithography. *Proc. Natl. Acad. Sci. U. S. A.* **2011**, *108*, 19521–19525.
- (16) Formanek, F.; Takeyasu, N.; Tanaka, T.; Chiyoda, K.; Ishikawa, A.; Kawata, S. Three-dimensional fabrication of metallic nanostructures over large areas by two-photon polymerization. *Opt. Express* **2006**, *14*, 800–809.
- (17) Cao, Y.-Y.; Takeyasu, N.; Tanaka, T.; Duan, X.-M.; Kawata, S. 3D metallic nanostructure fabrication by surfactant-assisted multiphoton-induced reduction. *Small* **2009**, *5*, 1144–1148.
- (18) Masui, K.; Shoji, S.; Asaba, K.; Rodgers, T. C.; Jin, F.; Duan, X.-M.; Kawata, S. Laser fabrication of Au nanorod aggregates microstructures assisted by two-photon polymerization. *Opt. Express* **2011**, *19*, 22786–22796.
- (19) Hu, Q.; Sun, X.-Z.; Parmenter, C. D. J.; Fay, M. W.; Smith, E. F.; Rance, G. A.; He, Y.; Zhang, F.; Liu, Y.; Irvine, D.; et al. Additive manufacture of complex 3D Au-containing nanocomposites by simultaneous two-photon polymerisation and photoreduction. *Sci. Rep.* **2017**, *7*, 17150.
- (20) Shukla, S.; Furlani, E. P.; Vidal, X.; Swihart, M. T.; Prasad, P. N. Two-photon lithography of sub-wavelength metallic structures in a polymer matrix. *Adv. Mater.* **2010**, *22*, 3695–3699.
- (21) Jonušauskas, L.; Lau, M.; Gruber, P.; Gökce, B.; Barcikowski, S.; Malinauskas, M.; Ovsianikov, A. Plasmon assisted 3D microstructuring of gold nanoparticle-doped polymers. *Nanotechnology* **2016**, *27*, 154001.
- (22) Tanaka, T.; Ishikawa, A.; Kawata, S. Two-photon-induced reduction of metal ions for fabricating three-dimensional electrically conductive metallic microstructure. *Appl. Phys. Lett.* **2006**, *88*, 081107.
- (23) Maruo, S.; Saeki, T. Femtosecond laser direct writing of metallic microstructures by photoreduction of silver nitrate in a polymer matrix. *Opt. Express* **2008**, *16*, 1174–1179.
- (24) Terzaki, K.; Vasilantonakis, N.; Gaidukeviciute, A.; Reinhardt, C.; Fotakis, C.; Vamvakaki, M.; Farsari, M. 3D conducting nanostructures fabricated using direct laser writing. *Opt. Mater. Express* **2011**, *1*, 586–597.
- (25) Hong, S.; Lee, J. S.; Ryu, J.; Lee, S. H.; Lee, D. Y.; Kim, D.-P.; Park, C. B.; Lee, H. Bio-inspired strategy for on-surface synthesis of silver nanoparticles for metal/organic hybrid nanomaterials and LDIMS substrates. *Nanotechnology* **2011**, *22*, 494020.
- (26) Aekbote, B. L.; Jacak, J.; Schütz, G. J.; Csányi, E.; Szegletes, Z.; Ormos, P.; Kelemen, L. Aminosilane-based functionalization of two-photon polymerized 3D SU-8 microstructures. *Eur. Polym. J.* **2012**, *48*, 1745–1754.
- (27) Focsan, M.; Craciun, A. M.; Astilean, S.; Baldeck, P. L. Two-photon fabrication of three-dimensional silver microstructures in microfluidic channels for volumetric surface-enhanced Raman scattering detection. *Opt. Mater. Express* **2016**, *6*, 1587–1593.
- (28) Fei, B.; Qian, B.; Yang, Z.; Wang, R.; Liu, W. C.; Mak, C. L.; Xin, J. H. Coating carbon nanotubes by spontaneous oxidative polymerization of dopamine. *Carbon* **2008**, *46*, 1795–1797.
- (29) Ahmed, S. R.; Kim, J.; Tran, V. T.; Suzuki, T.; Neethirajan, S.; Lee, J.; Park, E. Y. In situ self-assembly of gold nanoparticles on hydrophilic and hydrophobic substrates for influenza virus-sensing platform. *Sci. Rep.* **2017**, *7*, 44495.
- (30) Baker, C. O.; Shedd, B.; Tseng, R. J.; Martinez-Morales, A. A.; Ozkan, C. S.; Ozkan, M.; Yang, Y.; Kaner, R. B. Size control of gold nanoparticles grown on polyaniline nanofibers for bistable memory devices. *ACS Nano* **2011**, *5*, 3469–3474.
- (31) Quick, A. S.; Fischer, J.; Richter, B.; Pauloeuhl, T.; Trouillet, V.; Wegener, M.; Barner-Kowollik, C. Preparation of reactive three-dimensional microstructures via direct laser writing and thiol-ene chemistry. *Macromol. Rapid Commun.* **2013**, *34*, 335–340.
- (32) Grönbeck, H.; Curioni, A.; Andreoni, W. Thiols and Disulfides on the Au(111) Surface: The Headgroup–Gold Interaction. *J. Am. Chem. Soc.* **2000**, *122*, 3839–3842.
- (33) Dulkeith, E.; Morteani, A. C.; Niedereichholz, T.; Klar, T. A.; Feldmann, J.; Levi, S. A.; van Veggel, F. C. J. M.; Reinhoudt, D. N.; Möller, M.; Gittins, D. I. Fluorescence quenching of dye molecules near gold nanoparticles: radiative and nonradiative effects. *Phys. Rev. Lett.* **2002**, *89*, 203002.
- (34) Wiesbauer, M.; Wollhofen, R.; Vasic, B.; Schilcher, K.; Jacak, J.; Klar, T. A. Nano-anchors with single protein capacity produced with STED lithography. *Nano Lett.* **2013**, *13*, 5672–5678.
- (35) Wolfesberger, C.; Wollhofen, R.; Buchegger, B.; Jacak, J.; Klar, T. A. Streptavidin functionalized polymer nanodots fabricated by visible light lithography. *J. Nanobiotechnol.* **2015**, *13*, 27.
- (36) Wollhofen, R.; Axmann, M.; Freudenthaler, P.; Gabriel, C.; Röhl, C.; Stangl, H.; Klar, T. A.; Jacak, J. Multiphoton-Polymerized 3D Protein Assay. *ACS Appl. Mater. Interfaces* **2018**, *10*, 1474–1479.
- (37) Buchegger, B.; Kreutzer, J.; Axmann, M.; Mayr, S.; Wollhofen, R.; Plochberger, B.; Jacak, J.; Klar, T. A. Proteins on Supported Lipid Bilayers Diffusing around Proteins Fixed on Acrylate Anchors. *Anal. Chem.* **2018**, *90*, 12372–12376.
- (38) Huppa, J. B.; Axmann, M.; Mörtelmaier, M. A.; Lillemeier, B. F.; Newell, E. W.; Brameshuber, M.; Klein, L. O.; Schütz, G. J.; Davis, M. M. TCR-peptide-MHC interactions in situ show accelerated kinetics and increased affinity. *Nature* **2010**, *463*, 963–967.
- (39) Mayr, S.; Hauser, F.; Peterbauer, A.; Tauscher, A.; Naderer, C.; Axmann, M.; Plochberger, B.; Jacak, J. Localization Microscopy of Actin Cytoskeleton in Human Platelets. *Int. J. Mol. Sci.* **2018**, *19*, 1150.
- (40) Liu, Y.; Hou, W.; Sun, H.; Cui, C.; Zhang, L.; Jiang, Y.; Wu, Y.; Wang, Y.; Li, J.; Sumerlin, B. S.; et al. Thiol-ene click chemistry: a biocompatible way for orthogonal bioconjugation of colloidal nanoparticles. *Chem. Sci.* **2017**, *8*, 6182–6187.